Available online at www.sciencedirect.com
SCIENCE DIRECT®
Applied Surface Science 239 (2005) 410–423
applied surface science
www.elsevier.com/locate/apsusc

Hydrophobic recovery of UV/ozone treated poly(dimethylsiloxane): adhesion studies by contact mechanics and mechanism of surface modification

Attila Oláh[a,b], Henrik Hillborg[a], G. Julius Vancso[a,b,*]

[a]*Department of Materials Science and Technology of Polymers, MESA+ Institute for Nanotechnology, Faculty of Science and Technology, University of Twente, P. O. Box 217, 7500 AE, Enschede, The Netherlands*
[b]*Dutch Polymer Institute, P. O. Box 902, 5600 AX Eindhoven, The Netherlands*

Received 28 May 2004; accepted 2 June 2004
Available online 20 July 2004

Abstract

Silicone elastomers (Sylgard 184 and 170), based on poly(dimethylsiloxane) (PDMS), were surface treated by a combined exposure to UV and ozone. The effects of the treatments were analyzed as a function of time elapsed after stopping the treatments using different standard surface characterization techniques, such as water contact angle measurements, XPS and atomic force microscopy (AFM). However, the primary focus of this study was to apply the Johnson–Kendall–Roberts (JKR) contact mechanics approach to investigate PDMS samples prior to and following UV/ozone surface treatment. A gradual formation of a hydrophilic, silica-like surface layer with increasing modulus was observed with increasing UV/ozone exposure. A subsequent hydrophobic recovery after UV/ozone exposure was observed, as indicated by increasing contact angles. This supports the hypothesis that the hydrophobic recovery is mainly caused by the gradual coverage of a permanent silica-like structure with free siloxanes and/or reorientation of polar groups. PDMS containing a homogenously dispersed filler (Sylgard 184), exhibited a decreasing surface roughness (by AFM) when the oxidized surface region "collapsed" into a smooth SiO_x layer (final surface roughness <2 nm). PDMS containing heterogeneously distributed, aggregated filler particles (Sylgard 170), exhibited an increasing surface roughness with treatment dose, which was attributed to the "collapse" of the oxidized surface region thus exposing the contours of the underlying filler aggregates (final surface roughness ~140 nm). A dedicated device was designed and built to study the contact mechanics behavior of PDMS prior to, and following surface treatment. The value of the combined elastic modulus obtained for PDMS lens and semi-infinite flat surface system showed an increase in full agreement with the formation of a silica-like layer exhibiting a high elastic modulus (compared with untreated PDMS). The work of adhesion observed in JKR experiments exhibited an increasing trend as a function of treatment done in agreement with contact angle data. JKR experiments showed hydrophobic recovery behavior as anticipated from contact angle measurements. Single pull-off force measurements by JKR and numerical analysis of full-approach JKR curves were in quantitative agreement regarding practical work of adhesion values.

Keywords: JKR contact mechanics; Poly(dimethylsiloxane); Surface modification; Atomic force microscopy; Adhesion

* Corresponding author. Tel.: +31 53 489 2967; fax: +31 53 489 3823.
E-mail address: g.j.vancso@utwente.nl (G.J. Vancso).

0169-4332/$ – see front matter © 2004 Elsevier B.V. All rights reserved.
doi:10.1016/j.apsusc.2004.06.005

1. Introduction

Silicone elastomers based on poly(dimethylsiloxane) (PDMS), are widely used in various areas as diverse as high-voltage outdoor insulation [1,2], anti-fouling coatings [3], or biomedical applications [4]. The reason for this widespread use is related to an attractive combination of material properties, such as a hydrophobic surface, constant and high ductility over a wide range of temperatures, low toxicity, high electrical resistance, long-term endurance and flexible processing techniques. However, in many applications, a wettable PDMS surface would be of great value, for example in microfluidic devices [5], and in microcontact printing of hydrophilic polymers, or proteins, using PDMS stamps [6]. In the literature there is a large number of studies describing modifications of the intrinsically inert and hydrophobic PDMS surfaces. In order to change the surface energy and introduce various polar groups, corona discharges [7,8], UV-irradiation in combination with ozone [9–12] and oxygen plasma [13–20] treatments (among others) have been used. The oxygen plasma contains a complex mixture of high energy photons, electrons, ions, radicals and excited species. The species generated with high kinetic energy may cause surface sputtering effects. Due to the lack of high kinetic energy particles the UV/ozone treatment, which is part of the O_2 plasma treatment family, is considered to be milder than other high energy O_2 plasmas. For a deeper understanding of O_2 plasma surface treatments, the oxidation processes and their effect on PDMS surfaces have been extensively investigated using X-ray photoelectron spectroscopy (XPS), atomic force microscopy (AFM) and contact angle measurements by us and others [7,14–19,21–23]. The initial effects of all oxidative treatments listed above on PDMS includes a local incorporation of polar groups attached covalently to the exposed segments of PDMS in the surface region. The flexible chain dynamics is still maintained at these low degrees of oxidation, allowing molecular relaxation processes to occur. During these processes polar groups are turned into PDMS surface layers, thus effectively (and reversibly) decreasing the surface free energy [24]. This is reflected in essentially unchanged advancing water contact angles whereas significant reductions in receding water contact angle are observed when contact angle measurements are performed in an ambient environment [7,14,17,18]. Complementary XPS data indicates only a small degree of surface oxidation at these early stages of the oxidation process. This stage may last for a few seconds in a powerful oxygen plasma and up to tens of minutes for short-wave UV-treatments [19,25]. At higher doses the gradual conversion proceeds further, from the slightly oxidized PDMS structure with high segmental mobility into an inorganic silica-like structure. By XPS this is reflected by a rapid decrease of carbon content and increasing oxygen content, while the silicon content remained essentially constant [7,14–19]. Moreover, the binding energy of the Si 2p photoelectrons is shifted toward the value characteristic for Si in inorganic materials ($\sim$103.5 eV). After an initially rapid oxidation process the conversion of PDMS reached a saturation plateau, thus a complete conversion into SiO_2 did not occur [22]. These layers are often referred to as silica-like (SiO_x, $1 \leq x \leq 2$). The thickness of the corresponding SiO_x layers has been estimated to be between 10 and 160 nm [10,12,15,19]. The difference in reported thickness values is attributed to different treatment conditions and to variations in the surface analysis methods used. By AFM it has been shown that the surface roughness is decreasing during the treatment [22]. However, the surface roughness of the oxygen plasma treated PDMS also depends on the temperature, due to the difference in thermal expansion coefficient between bulk PDMS and the SiO_x layer formed at the surface treated. Complex surface structures can be created when these layers are subjected to temperature changes. For example, Bowden, Whitesides and others described a technique to form sinusoidal surface structures on the micrometer scale with patterned PDMS using temperature as an additional variable to oxygen plasma treatments [23]. Chan et al. showed that oxygen plasma exposure of silicone-containing polymer films at elevated temperatures resulted in buckled, or reticulated, surfaces exhibiting pattern motifs with sizes on the order of few micrometers [26]. We have used such ''buckled'' stamps to transfer etch-resistant poly(ferrocenylsilane) polymers as etch resists for soft lithography applications [27]. Due to a large difference in elastic modulus of the rigid top layer and the elastic bulk, the SiO_x layer formed may also form cracks upon mechanical stresses [18,19].

Generally, the hydrophilic surfaces of oxidized PDMS are not stable with time after exposure and a 'hydrophobic recovery' will gradually occur [7,13–19,25]. At low degrees of oxidation, as discussed previously, this recovery is caused by reversible relaxation processes of polar groups, whereas at sufficiently high doses another recovery process becomes dominating. This process is related to the diffusion of free low molar mass siloxanes to the surface through a porous, or cracked, silica-like layer, thereby reducing the free surface energy. These free siloxanes are intrinsically present in the polymer network, as well as formed by UV-induced chain scission reactions.

PDMS has become a widely used material for JKR adhesion measurements [28], since it fulfills the strict requirements demanded in corresponding studies for one of the contacting surfaces (e.g. lens), such as full elastic recovery and easy processing by casting into smooth and homogeneous surfaces. Moreover, chemical modification of the PDMS lens surface is possible without affecting its bulk properties [29]. This allows one to attach (physically or chemically) layers of (macro) molecules of interest for studies of contact mechanical behavior.

The JKR adhesion measurement is based on an elastomeric lens, which is gradually brought into contact with a (usually flat) substrate at a given rate and then retracted until separation of the surfaces occur. By the application of the JKR theory of contact mechanics the work of adhesion (W) and the combined elastic modulus (K) can be calculated according to:

$$a^3 = \frac{R}{K}\left[P + 3\pi WR + \sqrt{6\pi WRP + (3\pi WR)^2}\right] \quad (1)$$

and

$$\frac{1}{K} = \frac{3}{4}\left(\frac{1-\nu_1^2}{E_1} + \frac{1-\nu_2^2}{E_2}\right) \quad (2)$$

where R is the lens radius; a the radius of the instantaneous contact area; P the recorded external load; E_1, E_2 and ν_1, ν_2 are the elastic moduli and the Poisson ratios of the elastic bodies 1 and 2, respectively. In the last decades JKR contact mechanics has proven to be a sensitive technique to study surface-related phenomena such as interfacial free energies between solids in contact, surface free energies and work of adhesion. Mechanical (adhesive) contacts between different materials is a central issue for many applications covering moving devices, fastening by adhesives, or for coatings. Surface free energy characteristics for such applications are usually obtained from contact angle data. In addition to fundamental difficulties, like obtaining surface free energies of pure materials of interest (in vacuum) from such experiments, contact angles measured by liquids include by nature a different response as true mechanical contacts between solids. Thus to deliver relevant surface free energy data for mechanical applications, the JKR technique (and other related approaches) are the methods of choice allowing experiments between the two solid materials of interest and studies at their interphases in mechanical contact.

As mentioned, the measurement of adhesive and cohesive properties of thin films of various materials by contact mechanics can be achieved by pressing a PDMS lens, coated with a thin continuous layer of the desired material, against a substrate (the other ''participant'' of the mechanical contact of interest). A good wetting between the film of interest coated to the lens and the underlying PDMS is then of paramount importance. Oxygen plasma treatments are often used to increase the free surface energy of PDMS for improved attachment of specimen layers [29–33]. Self-assembled monolayers (SAM) of silanes [29] and thin polymer films [30,31,33], have been successfully coated on oxidized PDMS lenses. In these studies it was assumed that the changes induced by the surface oxidation of PDMS did not influence the thermodynamic characteristics of the sample material attached to the lens. However, as previously mentioned, a higher modulus SiO_x surface layer is gradually formed when exposing PDMS to plasmas. In previous JKR studies involving oxidized PDMS surfaces an increase of the calculated combined modulus has also been observed, but has not been correlated to the formation of a silica-like surface layer [29,32].

To the best of our knowledge, no specific research has been carried out to investigate the surface mechanical properties of the oxidized PDMS using JKR-type adhesion measurements. In this paper we present data on the formation of silica-like layers on cross-linked PDMS exposed to UV/ozone irradiation, observed by JKR mechanics. These measurements are correlated to data obtained by water contact angles, XPS and AFM in part previously published [40]. The JKR measurements confirm the gradual formation of a stable, high

modulus silica-like layer, on PDMS exposed to UV/ozone, with increasing treatment dose.

2. Experimental

2.1. Sample preparation

Sylgard 184 (Dow Corning), consisting of poly-(dimethylsiloxane) (PDMS) and a reinforcing silica filler was prepared by carefully mixing the precursors Sylgard 184A/184B at a ratio of 10:1 by mass [34]. Sylgard 170 (Dow Corning), consisting of PDMS, a reinforcing silica filler and low amounts (<1 wt.%) of zinc oxide and carbon black was prepared by carefully mixing the precursors Sylgard 170A/170B at a ratio of 1:1 by mass. The mixtures were subsequently degassed in a vacuum oven at ambient temperature. For the JKR adhesion measurements films and sphere-cap-like lenses were prepared. For lens preparation small drops (1–2 μl) of the mixed and degassed precursors were applied with a microsyringe onto glass microscope slides, which had previously been treated with 1H, 1H, 2H, 2H perfluorodecyltrichlorosilane to reduce adhesion. The curing reaction was carried out at 120 °C for 24 h. The residual polymers and oligomers not covalently bound to the elastomer networks in the lenses were removed by subsequent Soxhlet extraction for at least 24 h using *n*-hexane as solvent, boiled at 120 °C. After extraction the lenses were dried in a vacuum oven at ambient temperature and stored in glass vials until use. Glass and silicon substrates were cleaned using Piranha solutions (mixture of 1:4 of 30% H_2O_2 and 70% concentrated H_2SO_4) at ambient temperature, carefully rinsed several times in Millipore water and ethanol and finally dried in a stream of nitrogen gas. The PDMS precursors were then spin-coated onto the substrates using a Spincoater Model P6700 (Specialty Coating Systems Inc.). After spin-coating the films were cured at 120 °C for 24 h and stored individually in plastic containers [35]. The thickness of the PDMS films ranged within 830 ± 100 nm according to ellipsometry (a Plasmos SD 2002 ellipsometer was used at a wavelength of 632.8 nm at a fixed incident angle of 70°; the value of the refractive index n_f was assumed to be = 1.4). The PDMS films thus obtained were also used for X-ray photoelectron spectroscopy analysis, atomic force microscopy and water contact angle measurements.

2.2. UV/ozone treatments

The UV/ozone treatment of PDMS surfaces was performed in a commercial UV/ozone cleaner (Ultra-Violet Products PR-100). The apparatus contained a low-pressure mercury UV-light, generating UV-emissions at 185 nm (1.5 mW cm^{-2}) and 254 nm (15 mW cm^{-2}) wavelengths, respectively. The distance between the UV-source and the PDMS films was 20 mm. The nominal ozone steady-state concentration of 55 ppm was produced in a two-step photochemical process, initiated by the photolysis of molecular oxygen at 185 nm.

2.3. Water contact angle measurements

The advancing and receding contact angles (θ_a and θ_r) were measured with Millipore water (18.4 MΩ cm) as probe liquid, using a contact angle microscope (Data Physics, OCA 15 Plus) at room temperature. The advancing and receding contact angles were measured on both sides of the drop and on at least three different locations for each sample.

2.4. X-ray photoelectron spectroscopy (XPS)

XPS spectra were obtained by using a PHI Quantera X-ray Microprobe spectrometer utilizing Al Kα radiation (hv = 1496.6 eV). The power of the monochromatic X-ray source was 25 W. The angle between the X-ray beam and sample surface was 90° and the angle between the sample surface and the analyzer was 45°. Survey spectra to screen the atomic surface compositions were obtained at a pass energy of 224 eV. The high resolution spectra of the Si 2p peak were obtained at a pass energy of 112 eV, resulting in a resolution of 0.9 eV. The curve fitting of the Si 2p peak was carried out with a non-linear least-squares curve fitting program using a combination of Gaussian and Lorentzian functions (70:30%). As restrictions during the fitting, the Si 2p peak was fixed at 101.92 eV and the full width at half maximum (FWHM) was kept at 1.52 eV [36]. The binding energies were referenced to the C 1s binding energy of the hydrocarbon of the PDMS (285 ± 0.1 eV) [37].

2.5. Atomic force microscopy (AFM)

AFM measurements were carried out with a Nano-Scope III multimode AFM (Digital Instruments (DI), Santa Barbara). Tapping-mode scans were performed with untreated silicon cantilevers/tips (Nanosensors, Germany) at ambient conditions using a 100 μm^2 *x*-, *y*-range scanner. The values of root mean square roughness (R_q) of surfaces were calculated from 20×20 μm^2 sized height images. Since the roughness parameter is line-dependent and all height values are relative, no flattening and plane-fitting procedures were used. The surface roughness was measured around at least three different positions on each sample.

2.6. Contact mechanical measurements (JKR device)

Contact mechanical measurements were carried out using a custom built device (Fig. 1). A UV/ozone-treated PDMS lens was placed onto a glass microscopy slide and mounted in the device. A UV/ozone-treated PDMS coated glass slide was then firmly clamped into the sample holder frame and attached to a force transducer with a 25 g peak sensitivity (Thames-side Maywood Ltd.). The load cell was fixed on a movable stage of an XYZ table (Time and Precision Inds. Ltd.). The movement of the stage was monitored by a displacement transducer with an accuracy of 77.42 mV mm^{-1} (Omega Engineering Inc.). The movable stage was driven by a bipolar stepper motor with a resolution of $\sim$42 nm $step^{-1}$ in the vertical direction. The contact area between the PDMS lens and the PDMS film was continuously monitored by a CCD Camera (SONY XC-999P) through a custom made optical microscope utilizing a 10× magnification. The size of the field of view was 535×414 μm. The maximum diameter of the contact area was limited to 100 μm in order to keep the deformations within the elastic regime [38]. The values of the temperature (*T*) and relative humidity (RH) were monitored by a combined sensor (T&RH) with an accuracy of ±3.5% (Sensiron SHT 11). The signals from the load cell, displacement transducer, T&RH sensor and CCD camera were processed by a computer using a custom written LabVIEW™ software. Our device can be operated in a stepwise mode, or in continuous measurements. The measurements were carried out after at least 30 min equilibrating time after mounting the samples onto the sample holder stage. Contact mechanics measurements in sequence, on the same sample, were carried out after shifting the position of the film substrates under the lens

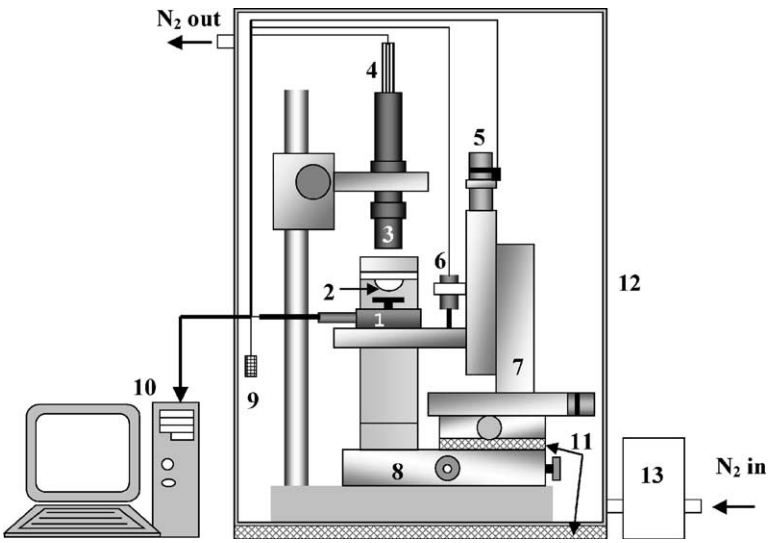

Fig. 1. The JKR device used to measure contact deformation between UV/ozone treated PDMS lenses and thin films. (1) Thin PDMS film substrates attached to the load cell. (2) PDMS lens. (3) Optical microscope. (4) CCD camera. (5) Stepper motor. (6) Displacement transducer. (7) XYZ table. (8) XY table. (9) Humidity and temperature sensor. (10) Computer. (11) Vibration damping rubber. (12) Glove box. (13) Humidity controller.

following approach-withdrawal cycles in order to ensure that each contact area on the PDMS film was only used once. Radii of the PDMS lenses were obtained using their side-view images captured under a conventional optical microscope, following after the JKR measurements. The values of the work of adhesion and combined elastic modulus were obtained by fitting the recorded advancing force–contact area relationship using the JKR theory by Eqs. (1) and (2) [28]. (Here, and later in this paper, work of adhesion is defined as practical work of adhesion, which can be different from thermodynamic, reversible work of adhesion due to energy dissipation processes taking place during the experiments.) The maximum adherence force was obtained as the lowest value of the retracting force–distance curve, prior to snap-off.

3. Results and discussion

3.1. Surface modification and analysis

The effect of the UV/ozone treatment time on the atomic surface composition of PDMS was assessed by X-ray photoelectron spectroscopy (XPS) within 6 h after the UV/ozone exposure. The results are summarized in Table 1. The theoretical atomic composition of PDMS, based on the repeat unit, is: 25% Si, 25% O and 50% C. For Sylgard 184 (see Table 1) a higher oxygen content was observed at the expense of carbon.

Table 1
Atomic surface composition of UV/ozone-exposed Sylgard 184 and 170 obtained by XPS

Exposure time (min)	Atomic composition (at.%)		
	Si	C	O
(a) Sylgard 184 obtained by XPS			
0	25.1	43.8	31.3
10	24.3	47.8	27.9
30	25.7	37.4	36.9
60	25.5	21.6	52.9
120	–	–	–
(b) Sylgard 170 obtained by XPS			
0	23.2	50.9	25.9
10	24.5	46.2	29.3
30	24.2	37.2	38.5
60	25.6	20.9	53.4
120	23.7	15.7	58.3

This may suggest a contribution from the silica-filler to the XPS spectra, even though previous studies of silica-filled PDMS led to the conclusion that the silica filler is rarely observed in the probed depth by XPS (~7–10 nm) [39]. For Sylgard 170, the higher carbon content obtained by XPS may indicate the presence of carbon black in the probed volume (Table 1). When exposed to UV/ozone, the carbon content decreased, whereas the oxygen content increased with increasing exposure time for both samples. The silicon content remained approximately constant between 24 and 26 at.%. The data suggests an increase in the average number of oxygen bonded to silicon, at the expense of the carbon content, i.e., the process of oxidative cross-linking within the probed depth can be postulated. The similarity of the oxidation rate between Sylgard 184 and 170, as indicated by the atomic surface composition changes (Table 1), suggests that the same oxidative mechanism was involved for both materials. High-resolution spectra for the Si 2p orbital peaks (observed for both types of PDMS) showed a peak broadening and a shift towards higher binding energies at ~103.6 eV (for a representative example see Fig. 2), which corresponds to the formation of a silica-like structure (SiO_x, $1 \leq x \leq 2$) in the surface region [7,16,37]. Even though this shift towards an ''inorganic'' Si environment increased with UV/ozone

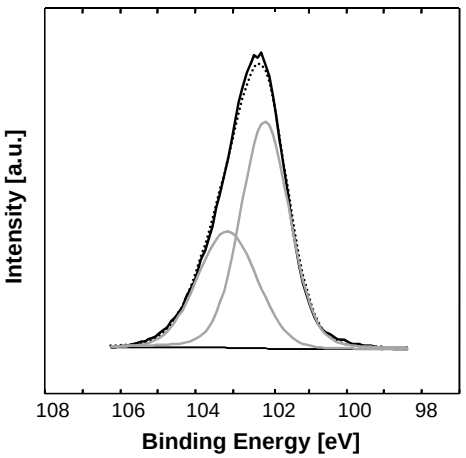

Fig. 2. Example of XPS curve resolution of the Si 2p of Sylgard 184, after exposure to 10 min UV/ozone. The peak at 101.9 eV corresponds to silicon in PDMS, while the peak at the higher binding energy (~103.6 eV) corresponds to oxidized silicon (SiO_x). The original (solid) and fitted (dotted) XPS signals are shown separately.

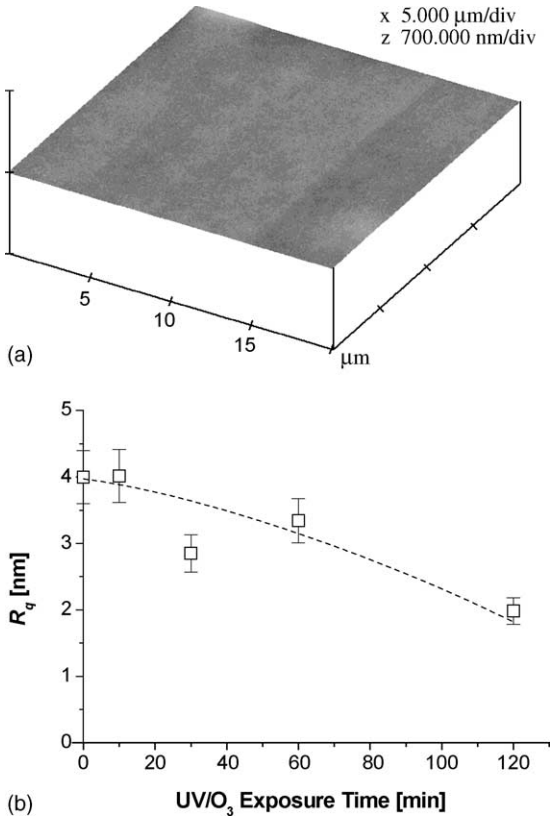

Fig. 3. (a) Representative AFM height image of the surface topography of Sylgard 184 after 60 min UV/ozone exposure (scan size: 20 × 20 µm^2, z-range: 700 nm div^{-1}). (b) Root mean square roughnesses (R_q) of Sylgard 184 as function of UV/ozone exposure time, obtained by AFM. The dashed line serves to guide the eye only.

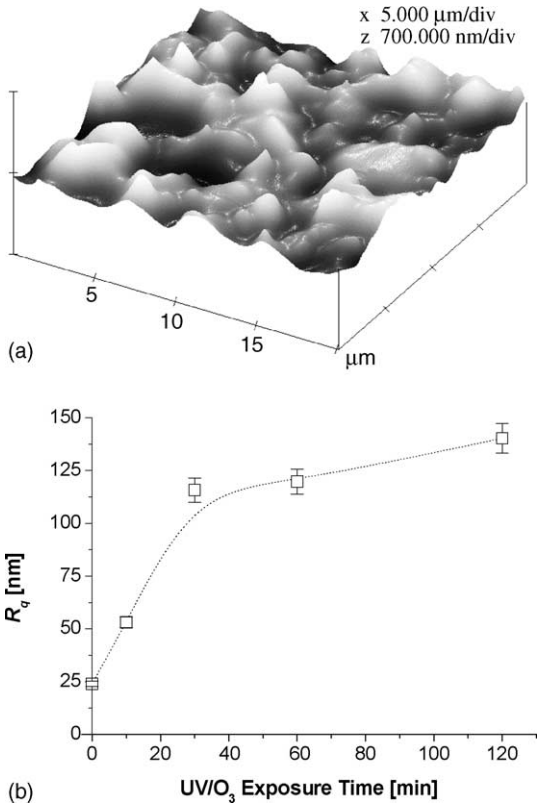

Fig. 4. (a) Representative AFM height image of the surface topography of Sylgard 170 after 60 min UV/ozone exposure (scan size: 20 × 20 µm^2, z-range: 700 nm div^{-1}). (b) Root mean square roughnesses (R_q) of Sylgard 170 as function of UV/ozone exposure time, obtained by AFM. The dashed line serves to guide the eye only.

exposure time, a contribution from PDMS at 101.9 eV remained visible. The remaining carbon content (Table 1) in combination with the high resolution spectra suggested that a full conversion into SiO_2 did not occur during UV/ozone treatments utilized in this study. The surface conversion process to silica-like layers may be limited by imperfect domains in the converted layers [40] or by migration of free siloxanes into the oxidized region [7,16] Lower conversions can also be an effect of underlying unconverted PDMS contributing to the signal, if the thickness of the SiO_x layer is lower than the effective sampling depth of XPS. Other details of the formation of the silica-like layer are summarized in a complementary study [40].

Even though both Sylgard 184 and 170 are based on PDMS, the difference in filler content and filler type greatly influenced the effect of the UV/ozone treatment on the surface roughness. Tapping-mode atomic force microscopy (AFM) revealed that sample of Sylgard 184 exhibited smooth, homogenous and featureless surfaces before and after exposure (Fig. 3a). The root mean square roughness (R_q) decreased with increasing UV/ozone exposure, from 4.0 ± 0.4 to 1.9 ± 0.2 nm (Fig. 3b) for a scan area of 20 × 20 µm^2. Vasilets et al. observed the same trend after exposing PDMS to UV/ozone [11]. Samples of Sylgard 170 exhibited a significantly rougher initial surface morphology of 24 ± 1.2 nm roughness, with roughness values increasing with exposure time (Fig. 4). This is most likely a result of the higher filler content of Sylgard 170 [41]. This effect was further investigated using low set point AFM tapping (e.g. high applied peak force, using a drive amplitude of 120 mV) of unexposed samples, thereby probing the filler distri-

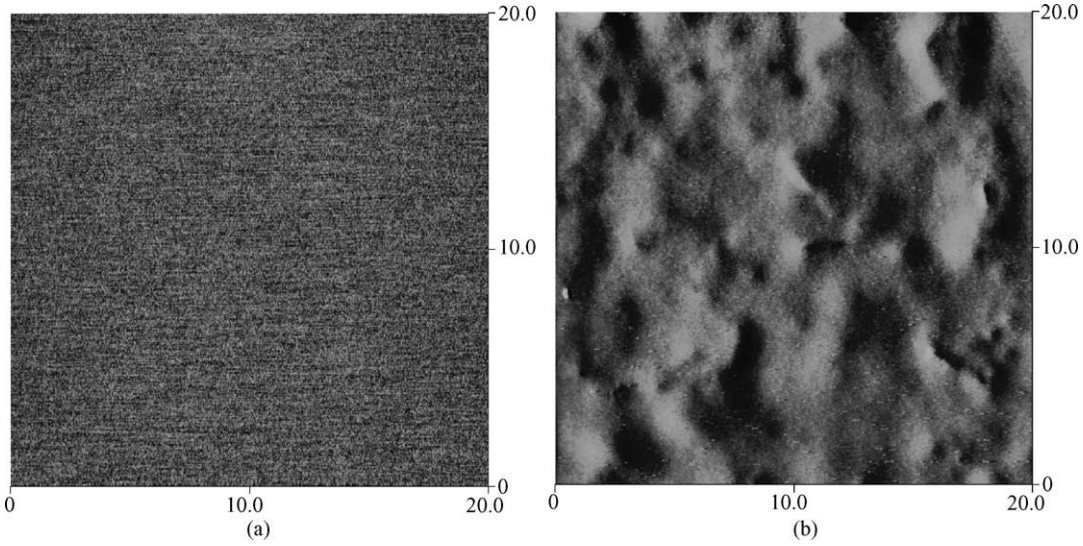

Fig. 5. AFM phase images (phase shift scale and tapping conditions were similar) showing the filler dispersion in (a) Sylgard 184 and (b) Sylgard 170 (scan size: 20 × 20 μm^2 and z-scale: 15°).

butions beneath the surface. AFM phase imaging showed that the Sylgard 184 specimen exhibited a sooth structureless image indicating homogeneously distributed silica filler particles (Fig. 5a), whereas the sample of Sylgard 170 exhibited large features interpreted as images of heterogeneous filler aggregates (Fig. 5b). We suggest that the decreased roughness of the Sylgard 184 with increasing UV/ozone exposure time is caused by the gradual formation of a smooth silica-like layer. During this oxidation process the PDMS in the exposed surface region collapses into a thinner, densified, silica-like layer. The same gradual formation and collapse of the silica-like layer should occur also for Sylgard 170, but here the large filler agglomerates become ''more exposed'' when the oxidized surface layer gradually collapses, resulting in an increasing surface roughness. It is interesting to note that the increase in surface roughness of Sylgard 170 appears to reach a plateau at approximately 100 nm roughness value for the scan size utilized (20 × 20 μm^2).

The effect of the UV/ozone exposure on hydrophobicity was assessed by water contact angle measurements (Fig. 6). Exposure times below 30 min caused a rapid reduction in the receding contact angles from 95–100 ± 2° to 45–65 ± 3°, whereas the advancing angles remained essentially unchanged for both Sylgard 184 and 170. The difference between the advancing and the receding contact angle is referred to as the *contact angle hysteresis* and depends on the roughness, chemical heterogeneity and molecular mobility (reorientation of functional groups) in the probed surface region [42]. Since the surface roughness was slightly decreasing for Sylgard 184 (i.e. no significant, roughness-related increase of the contact angle hysteresis could occur), the increased contact angle hysteresis after 2–30 min exposure suggests the introduction of polar groups (e.g. Si–OH), with high segmental mobility [39]. The increased segmental mobility could be contributed to surface damages caused by chain scission reactions. The increased contact angle hysteresis of Sylgard 170 is more difficult to assess since it is likely to be influenced both by surface oxidation and roughness changes. PDMS surfaces exposed to 60–120 min UV/ozone were rendered hydrophilic with advancing and receding contact angles ranging below 40°. The low contact angle hysteresis indicates a reduced molecular mobility in the surface region compared to the unexposed and partially oxidized surfaces (e.g. <60 min exposure) [39].

3.2. Hydrophobic recovery probed by contact angle measurements and contact mechanics

The hydrophobic stability of the oxidized surfaces after 10–120 min UV/ozone exposure was also

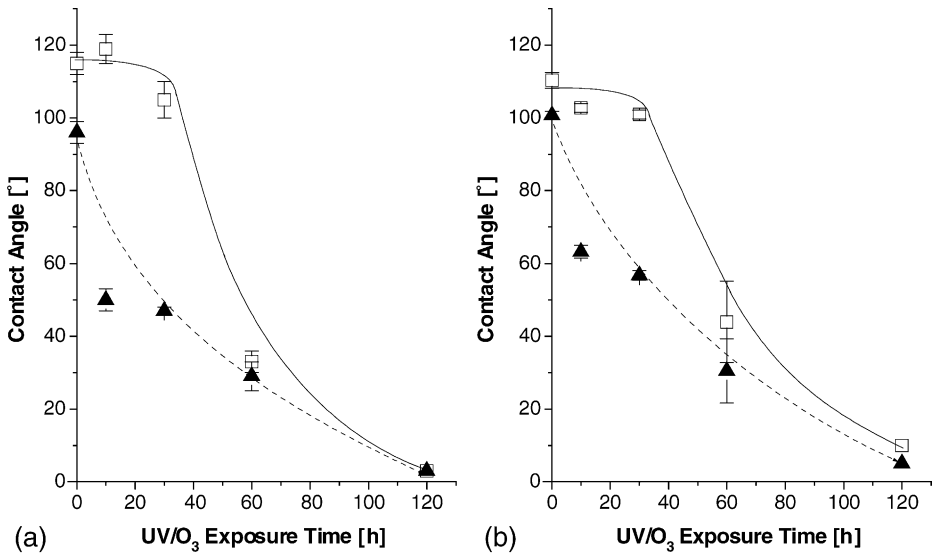

Fig. 6. Water contact angles as a function of UV/ozone exposure time. (a) Sylgard 184, and (b) Sylgard 170. (□) advancing and (▲) receding contact angles. The error bars indicate the standard deviation and the dashed and solid lines serve to guide the eye only.

assessed by water contact angle measurements (Fig. 7). Surfaces exposed to ≤30 min exposure exhibited only small changes. In a concurrent publication we suggested that lower doses of UV/ozone (≤30 min exposure) resulted in the gradual formation of a liquid-like layer, consisting of free oligomeric PDMS on top of a partly oxidized PDMS surface [40]. Chemical force microscopy (CFM) indicated that these surfaces were

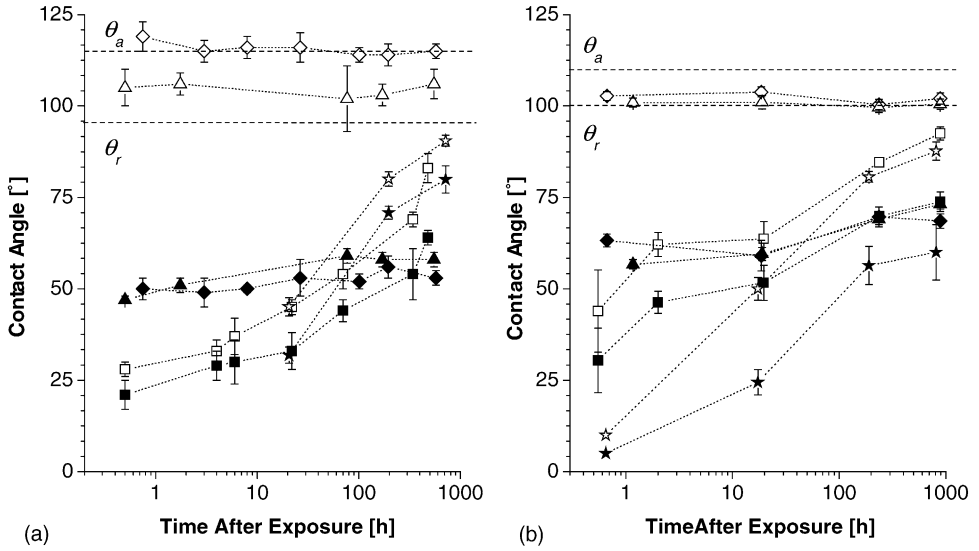

Fig. 7. Hydrophobic recovery of PDMS after 10–120 min exposure to UV/ozone: (a) Sylgard 184, (b) Sylgard 170. The dotted lines indicate the values of the initial advancing (θ_a) and receding contact angles (θ_r). Empty symbols: advancing contact angles, filled symbols: receding contact angles. Diamond: 10 min exposure; triangle: 30 min exposure; square: 60 min exposure. The horizontal, dashed lines indicate advancing and receding contact angles, respectively, of untreated PDMS.

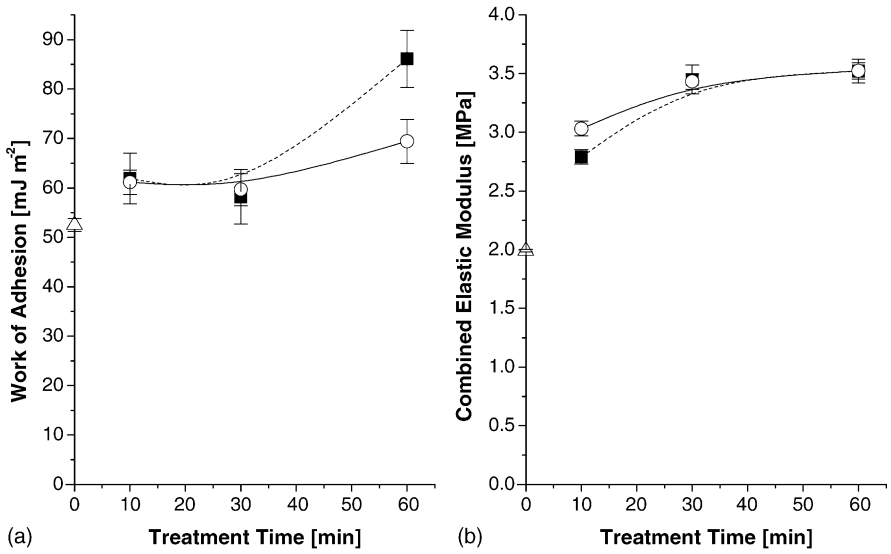

Fig. 8. (a) Calculated work of adhesion and (b) combined elastic modulus of Sylgard 184 after exposure to 10–60 min UV/ozone. (△) unexposed, (■) directly after exposure, (○) 8 days after exposure. The dashed and solid lines serve to guide the eye only.

homogenous on a sub-micrometer level, thus it was suggested that eventual surface heterogeneities could be masked by the free siloxanes [40]. Moreover CFM indentation mapping showed a decrease of the normalized modulus with time after exposure, indicating an enrichment of free siloxanes in the probed region [40].

The hydrophilic surfaces, formed after exposure to 60 and 120 min UV/ozone, exhibited an increasing hydrophobicity, as well as increasing contact angle hysteresis, with increasing time after exposure (Fig. 7). The dominating mechanism for this ''hydrophobic recovery'' is believed to be migration of free siloxanes from the bulk to the surface through a porous or cracked hydrophilic silica-like layer as discussed previously [7,14–16,40].

Several aspects discussing the formation of a silica-like layer during UV/ozone treatments and corresponding model have been described here and in other papers by us [40]. However, to our knowledge, no studies have been presented on the corresponding PDMS specimens obtained by contact mechanics. In order to assess applications, as mentioned in the introduction, such studies are anticipated to yield results more relevant for real use then surface physical-chemistry and other analytical investigations. Therefore, in the following section, we focus our attention on JKR contact mechanics behavior at the specimens analyzed in the preceding part by complementary analysis techniques. Utilizing contact mechanics, the surface treated PDMS samples were further investigated on a micrometer scale. JKR-type contact mechanical measurements were performed as a function of elapsed time after UV/ozone exposure (Figs. 8–10). The specimen consisting of Sylgard 170 initially exhibited a lower work of adhesion (43 mJ m^{-2}) than Sylgard 184 (53 mJ m^{-2}). Again this can be attributed to the higher initial surface roughness of Sylgard 170 as discussed in the preceding section [43]. When exposed to UV/ozone, the work of adhesion for the sample made of Sylgard 184 increased as a result of the introduction of polar groups in the surface region [44] (Fig. 8a), as previously indicated by the decreasing water contact angles. The calculated combined modulus (K) initially increased, but leveled off after more than 30 min exposure (Fig. 8b). We attribute the increased K to the formation of a silica-like surface layer. A ''hydrophobic recovery'' was also investigated by the work of adhesion. After 60 min UV/ozone treatment a decrease in the value of W_a was observed from 85 to 67 mJ m^{-2} during a period of 8 days (Fig. 8a). The combined elastic moduli were, however, stable with time after exposure (Fig. 8b). This gives further evidence for the formation of a permanent SiO_x

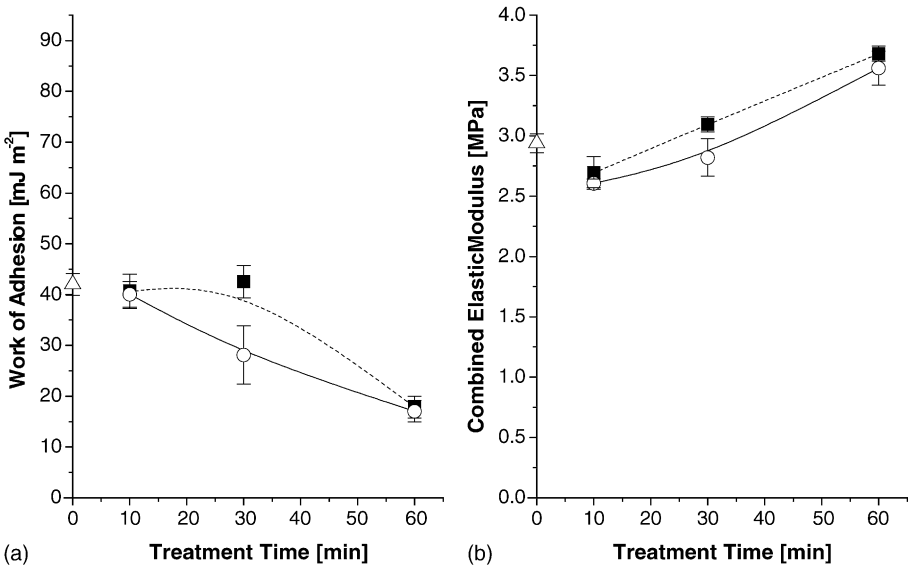

Fig. 9. (a) Calculated work of adhesion and (b) combined elastic modulus of Sylgard 170 after exposure to 10–60 min UV/ozone. (△) unexposed, (■) directly after exposure, (○) 8 days after exposure. The dashed and solid lines serve to guide the eye only.

surface layer which is stable with time after exposure, despite variations in the chemical composition of the outer layer as measured by contact angle, and XPS (hydrophobicity). The decreased work of adhesion with time of ageing following UV/ozone exposure may be caused by increasing amounts of free siloxanes escaping to the surface, acting as ''lubricant'' during the contact mechanics measurements. It has previously been shown that 60 min UV/ozone exposure of PDMS (Sylgard 184) led to the formation of a hydrophilic silica-like structure [40]. CFM mapping revealed a laterally heterogeneous structure on a

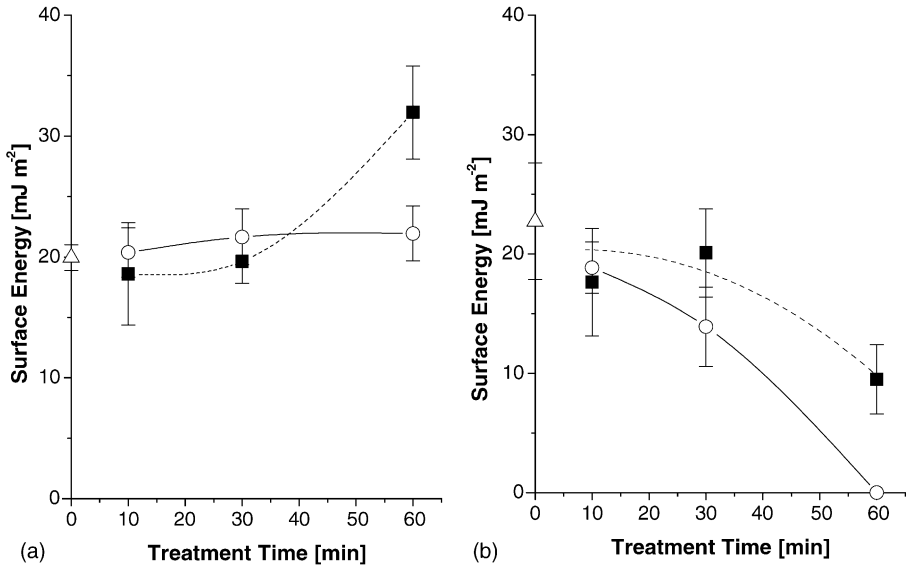

Fig. 10. Surface free energy of UV/ozone-treated PDMS calculated from the maximum adherence (pull-off) force. (a) Sylgard 184, and (b) Sylgard 170. (△) unexposed, (■) directly after exposure, (○) 8 days after exposure. The dashed and solid lines serve to guide the eye only.

<50 nm scale. Since the JKR measurements presented probe surface properties on the micrometer scale, such sub-micrometer structures may be difficult to detect by this technique.

After 10 min UV/ozone exposure of Sylgard 170 no significant change in work of adhesion occurred (Fig. 9a). After 30 min exposure, the work of adhesion initially remained unchanged, but then decreased with time after exposure, from 43 down to 28 mJ m^{-2}. About 60 min UV/ozone treatment resulted in an even larger reduction in the work of adhesion, down to 16 mJ m^{-2}. This value remained stable with the time elapsed after exposure. The increase in combined elastic modulus of Sylgard 170 was significantly lower, compared to Sylgard 184 (Fig. 9b) for comparable treatment dose. During the JKR measurements, the contact area of Sylgard 170 exhibited a ''rough'' appearance of contact area by optical observations, and an increasing number of small sized inclusions with increasing exposure time, whereas the contact area of Sylgard 184 remained homogenous throughout the measurements. The effect of the surface roughness on work of adhesion has been investigated previously for PDMS, where it was concluded that a critical modulus (E^*) determines the behavior of the system [45,46]. If $E \ll E^*$, a homogenous and complete contact area is obtained. An increase in surface roughness of the low modulus material results in an increasing contact area and an increasing value of W_a. For solids where $E > E^*$, an increase in surface roughness results in a reduced contact area and subsequently a decreased W_a [47]. We suggest that the observed reduction in work of adhesion of Sylgard 170 was a result of a decreasing contact area, caused by the increase in surface roughness and modulus.

In Fig. 10, the surface free energies, calculated from the maximum adherence (pull-off) forces upon withdrawal of the PDMS lenses from the PDMS films are presented. The data exhibit the same trends as the work of adhesion obtained from the JKR theory presented in Figs. 8 and 9. Compared to the work of adhesion data, the relative increase in surface free energy is lower, which can be explained by assuming that the oxidized surfaces are more or less coated with free siloxanes. The molecules of free siloxanes act as effective lubricants, thereby reducing the pull-off forces upon withdrawal. Thus the pull-off data appear to be more sensitive to surface contamination, compared to the work of adhesion obtained by contact area *versus* force at increasing contact. Very low, or even zero pull-off forces were observed performing JKR experiments directly after 60 min of UV/ozone treatment of Sylgard 170, as a result of the high surface roughness.

4. Conclusions

The effect of UV/ozone exposure on two different silicone elastomers (Sylgard 184 and 170), both based on poly(dimethylsiloxane), was investigated using surface characterization techniques ranging from continuum scale (water contact angle measurements and XPS) to the micrometer scale (JKR contact mechanics and AFM). Water contact angle measurements and XPS indicated the formation of a hydrophilic silica-like (SiO_x) layer after 60 min UV/ozone exposure. The increased modulus of this layer was reflected in an increased combined elastic modulus by JKR contact mechanics. Shorter exposure times (<60 min) resulted in an increased contact angle hysteresis as a result of decreasing receding contact angles while the advancing angles remained essentially unchanged. This indicated the presence of an oxidized surface with high segmental mobility, even though the increase in combined elastic modulus in combination with XPS data also suggested the presence of an increased oxidative cross-linking in the surface region. The surface roughnesses of the silica-like layers were found to be dependent on the filler size/content in the exposed material. PDMS containing a homogenously dispersed filler (Sylgard 184), exhibited a decreased surface roughness when the oxidized surface region collapsed into a very smooth SiO_x layer (final surface roughness <2 nm). PDMS containing a heterogeneously aggregated filler (Sylgard 170), exhibited an increasing surface roughness, probably since the collapsing oxidized surface region exposed more of the underlying filler aggregates (final surface roughness ~150 nm) [24b].

The subsequent hydrophobic recovery after UV/ozone exposure was observed on both the continuum scale by increasing contact angles as well as on the micrometer scale by a decreasing work of adhesion according to the JKR theory. The increase in combined elastic modulus obtained by the JKR model remained

constant with time after exposure. This result supports the hypothesis that the hydrophobic recovery is mainly caused by the gradual coverage of a permanent silica-like structure with free siloxanes and/or reorientation of polar groups. A direct comparison between the surface properties of Sylgard 184 and 170 was difficult to perform due to the large differences in surface roughness for the two elastomers.

Acknowledgements

The authors gratefully acknowledge financial support from the Dutch Polymer Institute (project no: 182) (A.O.) and the Swedish Foundation for International Cooperation in Research and Higher Education in the form of a post-doctoral scholarship (PD 2001-237) (H.H.). Dr. Holger Schönherr is thanked for the many stimulating discussions and for his help with atomic force microscopy.

References

[1] J. Kim, M.K. Chaudhury, M.J. Owen, IEEE. Trans. Dielectr. Electr. Insul. 6 (1999) 695.
[2] H. Hillborg, U.W. Gedde, IEEE Trans. Dielectr. Electr. Insul. 6 (1999) 703.
[3] J.K. Pike, T. Ho, K. Wynne, J. Chem. Mat. 8 (1996) 856.
[4] Y. Ikada, Biomaterials 15 (1994) 725.
[5] M. Koch, A. Evans, A. Brunnschweiler, Microfluidic Technology and Applications, Baldock, Research Studies Press, Hertfordshire, 2000.
[6] C. Donzel, M. Geissler, A. Bernard, H. Wolf, B. Michel, J. Hilborn, E. Delamarche, Adv. Mater. 13 (2001) 1164.
[7] H. Hillborg, U.W. Gedde, Polymer 19 (1998) 1991.
[8] M. Tirrell, A.V. Pocius, D.J. Kinning, D.J. Yarusso, B. Thakkar, V.S. Mangipudi, Plastics Eng. 53 (1997) 31.
[9] T.S. Phely-Bobin, R.J. Muisener, J.T. Koberstein, F. Papadimitrakopoulos, Adv. Mater. 12 (2000) 1257.
[10] M. Ouyang, C. Yuan, R.J. Muisener, A. Boulares, J.T. Koberstein, Chem. Mater. 12 (2000) 1591.
[11] V.N. Vasilets, K. Nakamura, Y. Uyama, S. Ogata, Y. Ikada, Polymer 39 (1998) 2875.
[12] C.L. Mirley, J.T. Koberstein, Langmuir 11 (1995) 1049.
[13] D.B.H. Chua, H.T. Ng, S.F.Y. Li, Appl. Phys. Lett. 76 (2000) 721.
[14] J.L. Fritz, M.J. Owen, J. Adhes. 54 (1995) 33.
[15] M.J. Owen, P.J. Smith, J. Adhes. Sci. Technol. 8 (1994) 1063.
[16] A. Tóth, I. Bertóti, M. Blazsó, G. Bánhegyi, A. Bognár, P. Szaplonczay, J. Appl. Polym. Sci. 52 (1994) 1293.
[17] M. Morra, E. Occhiello, R. Marola, F. Garbassi, P. Humphrey, D. Johnson, J. Colloid Interf. Sci. 137 (1990) 11.
[18] H. Hillborg, M. Sandelin, U.W. Gedde, Polymer 42 (2001) 7349.
[19] H. Hillborg, J.F. Ankner, U.W. Gedde, G.D. Smith, H.K. Yasuda, K. Wikström, Polymer 41 (2000) 6851.
[20] I. Korczagin, S. Golze, M.A. Hempenius, G.J. Vancso, Chem. Mater. 15 (2003) 3663.
[21] E.P. Everaert, H.C. VanderMei, H.J. Busscher, J. Adhes. Sci. Technol. 10 (1996) 351.
[22] M. Ouyang, R.J. Muisener, A. Boulares, J.T. Koberstein, J. Membr. Sci. 177 (2000) 177.
[23] (a) N. Bowden, W.T.S. Huck, K.E. Paul, G.M. Whitesides, Appl. Phys. Lett. 75 (1999) 2557;
(b) F. Katzenberg, Macromol. Mater. Eng. 286 (2001) 26.
[24] (a) M. Morra, E. Occhiello, R. Marola, F. Garbassi, P. Humphrey, D.J. Johnson, Colloid Interf. Sci. 137 (1990) 11;
(b) D. Trifonova, H. Schönherr, L. van der Does, P.J.P. Janssen, J.W.M. Noordermeer, G.J. Vancso, Rubber Chem. Technol. 72 (1999) 862.
[25] J. Kim, M.K. Chaudhury, M.J. Owen, J. Colloid Interf. Sci. 226 (2000) 231.
[26] V.Z.H. Chan, E.L. Thomas, J. Frommer, D. Sampson, R. Campbell, D. Miller, C. Hawker, V. Lee, R.D. Miller, Chem. Mater. 10 (1998) 3895.
[27] R.G.H. Lammertink, M. Peter, M.A. Hempenius, G.J. Vancso, PMSE Preprints 223 (2002) 262.
[28] K.L. Johnson, K. Kendall, A.D. Roberts, Proc. R. Soc. Lond. A Ser. A 324 (1971) 301.
[29] M.K. Chaudhury, G.M. Whitesides, Langmuir 7 (1991) 1013.
[30] M. Tirrell, Langmuir 12 (1996) 4548.
[31] V.S. Mangipudi, E. Huang, M. Tirrell, A.V. Pocius, Macromol. Symp. 102 (1996) 131.
[32] M. Rundlöf, M. Karlsson, L. Wågberg, E. Poptoshev, M. Rutland, P.J. Claesson, Colloid Interf. Sci. 230 (2000) 441.
[33] L. Li, V.S. Mangipudi, M. Tirrell, A.V. Pocius, in: B. Bushan (Ed.), Fundamentals of tribology and bridging the gap between the macro- and micro/nanoscales, Kluwer A.P., 2001, 305.
[34] The PDMS networks of Sylgard 184 and Sylgard 170 are formed by a hydrosilylation reaction between vinyl-terminated oligomeric dimehtylsiloxanes and a methylhydrosiloxane using a platinum complex as catalyst.
[35] The PDMS films on the silicon substrates were not extracted since this caused the films to delaminate from the substrates.
[36] A Full Width at Half Maximum (FMHM) of 1.52 was obtained fitting the Si 2p peak of unexposed Sylgard 184 using a single peak.
[37] G. Beamson, D. Briggs, High Resolution XPS of Organic Polymers: The Scienta ESCA300 Database, Wiley, Chichester, 1992.
[38] P. Chin, R.L. McCullough, W.L. Wu, J. Adhes. 64 (1997) 145.
[39] K. Efimenko, W.E. Wallace, J. Genzer, J. Colloid Interf. Sci. 254 (2002) 306.
[40] H. Hillborg, N. Tomczak, A. Oláh, H. Schönherr, G.J. Vancso, Langmuir 20 (2004) 785.

[41] The higher filler content is reflected in the higher density of Sylgard 170 (1.35 g cm^{-3}), compared to Sylgard 184 (1.05 g cm^{-3}).
[42] (a) S. Wu, Polymer Interfaces and Adhesion, M. Dekker Inc., 1982, 25 pp.;
(b) H. Yasuda, Plasma Polymerization, Academic Press, Orlando, 1985.
[43] L.H.G.J. Segeren, B. Siebum, F.G. Karssenberg, J.W.A. Van den Berg, G.J. Vancso, J. Adhes. Sci. Technol. 16 (2002) 793.
[44] The obtained W_a may however be reduced by the presence of a partial coverage of free siloxanes on the oxidized surfaces, thus reducing the amount of access able polar groups.
[45] H.C. Kim, T.P. Russell, J. Polym. Sci. Pt. B: Polym. Phys. 39 (2001) 1848.
[46] J.P. Pickering, PhD Thesis, University of Twente, Enschede, 2000, 191 pp.
[47] K.N.G. Fuller, D. Tabor, Proc. R. Soc. Lond. A A345 (1975) 327.